REPORT DOCUMENTATION PAGE

Form Approved
OMB No. 0704-0188

1. REPORT DATE *(DD-MM-YYYY)*
18-01-2003

2. REPORT TYPE
Technical Paper

3. DATES COVERED *(From - To)*

4. TITLE AND SUBTITLE

3-D Computation of Surface Sputtering and Redeposition Due to Hall Thruster Plumes

5a. CONTRACT NUMBER

5b. GRANT NUMBER

5c. PROGRAM ELEMENT NUMBER

6. AUTHOR(S)

J.M. Fife, M.R. Gibbons, W.A. Hargus[1] D.B. VanGilder, D.E. Kirtley[2]

5d. PROJECT NUMBER
4847

5e. TASK NUMBER
0052

5f. WORK UNIT NUMBER

7. PERFORMING ORGANIZATION NAME(S) AND ADDRESS(ES)

[1]Air Force Research Laboratory (AFMC)
AFRL/PRSS
1 Ara Road
Edwards AFB, CA 93524-7013

[2]ERC, Inc.
10 E. Saturn Blvd.
Edwards AFB, CA 93524-7680

8. PERFORMING ORGANIZATION REPORT NUMBER
AFRL-PR-ED-TP-2002-319

9. SPONSORING / MONITORING AGENCY NAME(S) AND ADDRESS(ES)

Air Force Research Laboratory (AFMC)
AFRL/PRS
5 Pollux Drive
Edwards AFB CA 93524-7048

10. SPONSOR/MONITOR'S ACRONYM(S)

11. SPONSOR/MONITOR'S NUMBER(S)
AFRL-PR-ED-TP-2002-319

12. DISTRIBUTION / AVAILABILITY STATEMENT

Approved for public release; distribution unlimited.

13. SUPPLEMENTARY NOTES

14. ABSTRACT

15. SUBJECT TERMS

16. SECURITY CLASSIFICATION OF:			**17. LIMITATION OF ABSTRACT**	**18. NUMBER OF PAGES**	**19a. NAME OF RESPONSIBLE PERSON**
					Leilani Richardson
a. REPORT	**b. ABSTRACT**	**c. THIS PAGE**	A		**19b. TELEPHONE NUMBER** *(include area code)*
Unclassified	**Unclassified**	**Unclassified**			(661) 275-5015

← DTS

MEMORANDUM FOR PRS (In-House/Contractor Publication)

FROM: PROI (STINFO) 23 Dec 2002

SUBJECT: Authorization for Release of Technical Information, Control Number: **AFRL-PR-ED-TP-2002-319**
J.M. Fife; M.R. Gibbons; W.A. Hargus, et al., "3-D Computation of Surface Sputtering and Redeposition Due to Hall Thruster Plumes"

0792

International Electric Propulsion Conference **(Statement A)**
(Toulouse, France, 17-21 March 2003) (Deadline: 15 Jan 2003)

3-D Computation of Surface Sputtering and Redeposition Due to Hall Thruster Plumes

J. M. Fife, M. R. Gibbons, and W. A. Hargus
U.S. Air Force Research Laboratory
Edwards AFB, CA

D. B. VanGilder and D. E. Kirtley
ERC, Inc.
Edwards AFB, CA

L. K. Johnson
Jet Propulsion Laboratory
Pasadena, CA

A 3-D computational plasma interaction modeling system is being developed to predict the interaction of electric propulsion plumes with surfaces. The system, named COLISEUM, is designed to be flexible, usable, and expandable, allowing users to define surfaces with their choice of off-the-shelf 3-D solid modeling packages. These surfaces are then loaded into COLISEUM, which calculates plasma expansion from electric thrusters using a variety of functional modules. Functional modules are interchangeable, and can range from simple (collisionless ray tracing) to complex (PIC-DSMC). Surface interaction parameters such as ion flux, ion energy, sputtering, and re-deposition are computed. Development to date has progressed to include the two simplest functional modules: PRESCRIBED_PLUME, which imports and superimposes a plume distribution, and RAY, which performs ray tracing of flux from point sources. This paper presents a new COLISEUM algorithm for calculating equilibrium re-sputtering and re-deposition of materials. This algorithm enables calculation of net deposition and sputtering of surfaces inside HET test facilities as well as in the space environment. Two cases are presented – one for a laboratory experiment in which sputtering and redeposition were measured, and another in which sputtering and redeposition on a generalized geosynchronous spacecraft is predicted.

Introduction

Several EP devices are currently being evaluated for use onboard U.S. commercial and military spacecraft. One of the most promising for near-term use is the Hall-effect thruster (HET). Over 120 HETs have flown on Russian spacecraft, where typical flight units have specific impulses around 1600 seconds and efficiencies near 50%.[1] HETs operate by generating a stationary xenon plasma inside an annular channel. Strong radial magnetic fields are applied which impede electron motion, but allow ions to accelerate axially out of the device with velocities around 20 km/s (energies of around 300 eV).

High-energy HET exhaust ions may erode (sputter) surfaces on which they impinge. In addition, this sputtered material may be re-deposited on other spacecraft surfaces. These issues, and others, such as electromagnetic interference and spacecraft charging, cause some concern for spacecraft designers who want the maneuverability EP offers but do not want increased risk.

Efforts are underway to accurately quantify some of the risks associated with integration of EP with spacecraft, including surface erosion and re-deposition. Work has been done to computationally model expansion of HET plumes.[2] Additionally, Gardner et al. have developed Environment Work Bench (EWB), a code that calculates sputtering of spacecraft surfaces by superimposing pre-computed EP plumes onto spacecraft geometries.[3,4] However, existing codes do not self-consistently calculate the plume expansion with 3-D surface sputtering in a usable, flexible way.

The Air Force Research Laboratory is leading development of a new software package named COLISEUM, which is capable of self-consistently modeling plasma propagation and interactions with arbitrary 3-D surfaces. Three important requirements have been placed on COLISEUM: It must be USABLE, FLEXIBLE, and EXPANDABLE.

USABLE means a typical engineer is able to set up and run a typical low-fidelity case in less than one day with less than three days training.

FLEXIBLE means COLISEUM is able to simulate at least three important cases: a) a single spacecraft, b) multiple spacecraft in formation, and c) laboratory conditions (e.g. the interior of a vacuum test facility). Simulating laboratory conditions is very important for two reasons. First, since there is very little on-orbit data for EP thrusters, ground-based tests must be relied upon for the bulk of code validation.

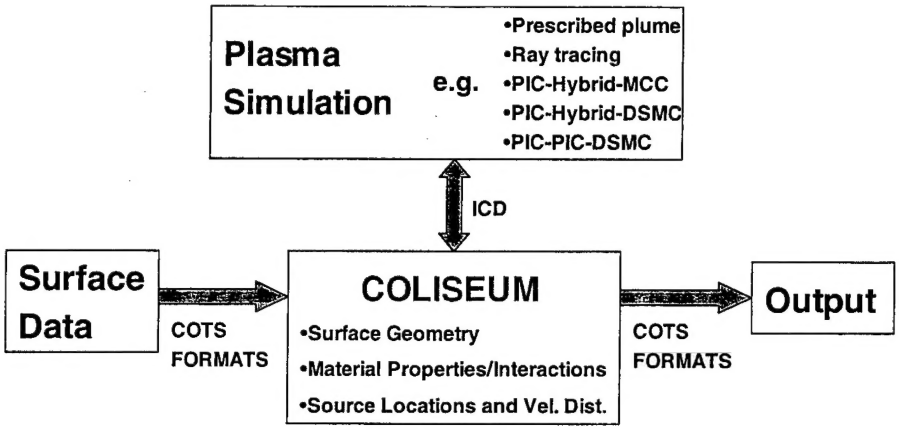

Fig. 1 Architecture for using various interchangeable plasma simulation techniques with the same 3-D surface geometry.

Second, by modeling the laboratory conditions, COLISEUM can help engineers interpret lab measurements.

In addition to being able to simulate multiple geometries, COLISEUM is flexible in its use of plasma simulation algorithms. Problem set-up and geometry definition is preformed once. Then, the user may select from a set of interchangeable plasma simulation algorithms to perform the solution. If low run-time is desired, a low-fidelity technique can be selected such as ray tracing. For higher fidelity (at the cost of longer run-time), something like Particle-In-Cell (PIC) can be used.

EXPANDABLE means COLISEUM can be easily expanded to incorporate new plasma simulation algorithms, new capabilities, or improved efficiency. Furthermore, as new plasma simulation algorithms are added, old ones will continue to function.

Approach

Fig. 1 shows how COLISEUM integrates with a set of various interchangeable plasma simulations. In general, COLISEUM can be viewed as a toolbox or framework in which 3-D plasma simulations can be quickly integrated. Common calculations (such as those related to surfaces, material properties, and flux sources) are standardized, grouped, and provided as a resource library (data and subroutines) to each simulation. This resource library takes the form of a `.lib` file that users link with their set of plasma simulation routines.

From a code architecture standpoint, COLISEUM has been designed as a core library, plus a collection of plasma simulation modules, each with a specific approach for calculating plasma expansion.

Plasma simulation modules are the primary components of COLISEUM. They calculate plasma propagation on the volume domain. They contain algorithms, such as ray tracing, fluid, PIC, DSMC, or hybrids thereof, which perform a solution subject to pre-set boundary conditions. Plasma simulation modules are interchangeable. They all conform to a specific Interface Control Document (ICD) – they have specific inputs, outputs, and resources available to them.

The core coliseum library functions support tasks common to all types of plasma simulations. They handle boundary conditions, and provide support to plasma simulation modules. They act as a toolbox or collection of resources. It is the core coliseum functions and data structures that make up the COLISEUM resource library.

The purpose of the modular design is to give COLISEUM flexibility and expandability. A large number of plasma simulation modules are desired to allow flexibility in solving a variety of different problems. The ICD is, therefore, very important, because it describes for authors of plasma simulation modules a) what inputs and boundary conditions must be recognized, b) what outputs are expected, and c) what core COLISEUM resources are available. The ICD and core COLISEUM resource library may be distributed to outside groups so that COLISEUM can be expanded through addition of new plasma simulation modules.

Surfaces

Surfaces are modeled in finite-element fashion as contiguous triangular elements joined at the vertices (nodes). COLISEUM does not generate 3-D geometries or surfaces; instead, it imports them from other software.

Users create custom geometries using almost any mainstream commercial 3-D solid modeling package. Then, they use finite element analysis software to mesh the surface of their geometry as if they were going to perform a structural analysis using thin shells. The user then saves the meshed surface file in ANSYS format, which is readable by COLISEUM. ANSYS finite element format was chosen because it is widely supported by finite element packages.

This concept of separating the surface geometry definition from the plasma calculation has proven very successful. It greatly reduced development time and cost by eliminating the need for a separate surface definition module. It allows users to choose which software to use in defining geometries. And, users can import into COLISEUM geometries that have already been defined for other reasons (structural, thermal, etc.).

Components

The user may construct a database of surface components that is read by COLISEUM. The database contains, at a minimum, the name of each component appearing on a surface geometry. Typically, the component database also contains a component reference number and a material name. The component reference number connects the component in the database to the surface geometry. Users mark surface components during geometry/surface definition using their finite element software. They simply set the elastic modulus of the surface component to be equal to the material reference number. This value appears in the ANSYS file, where COLISEUM reads it. The material name field links the component database to the material database.

Material Properties

The user constructs a database of materials that is read by COLISEUM. The database contains, at a minimum, each material name. The plasma simulations RAY and PRESCRIBED_PLUME require, in addition to material name, molecular weights, and charges (in the case of ions).

The user also provides a second database, a materials interaction database. This database contains the sputter yield coefficients and sticking coefficients of one material interacting with the other, e.g. between Xe^+ and Kapton.

Sources

Sources are modeled as having a specific velocity distribution that is a function of position on the surface, of three-dimensional velocity space, and of time. A collection of commands allows the user to either specify one of a set of pre-defined source types (Hall thruster, mono-energetic, half-Maxwellian, etc.), or their own user-defined source type (which must be coded and linked with the core COLISEUM library).

This method is extremely descriptive and general. Plasma simulation modules may treat the source distribution function in various ways. For instance, a plasma simulation module could be written to treat the source element a single point source for ray tracing purposes. Alternately, particle methods could sample from the velocity distribution and introduce particles randomly over the full element surface. Therefore, this choice of source definition methods gives COLISEUM great flexibility.

Plasma Simulation

Currently, two modules have been written. The first, PRESCRIBED_PLUME, allows the user to import a previously calculated or measured plume field. This plume is superimposed over the user's surface geometry. Plasma densities, fluxes, and sputter rates are then calculated at each surface node.

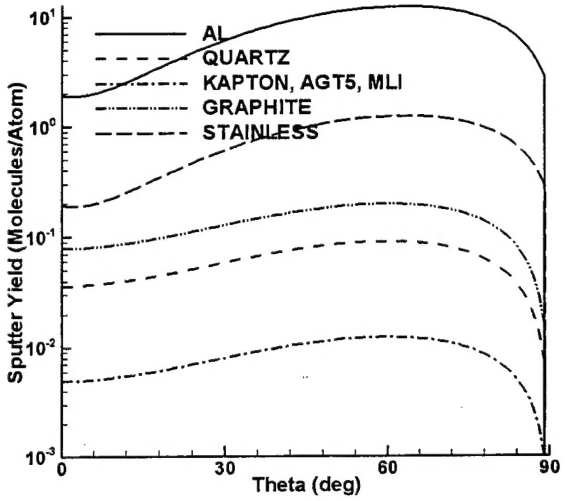

Fig. 2. Models of sputter yield versus incidence angle for Xe+ at 300eV.

The second module, RAY, uses ray tracing to calculate the flux from all sources onto all surface nodes. Once again, density, flux, and sputter rate are calculated.

Future modules will incorporate statistical kinetic methods for plasma calculation such as PIC and DSMC. Plans also include development of kinetic algorithms for use on unstructured meshes, adaptive meshes, and domain decomposition. Primarily, these techniques will be incorporated to add flexibility to the simulation. For instance, domain decomposition will allow the domain to be broken into smaller sub-domains, each potentially having different algorithms, depending on local parameters as the Debye length or mean free path.

Sputtering and Redeposition

The material interaction database can support multiple surface sputtering models. Currently, three models are implemented: a) constant yield, b) a model by Roussel et al.[5] (also used by Gardner et al.[3]), and c) a model by Kannenberg[6]. In this paper, sputtering is modeled for Xe+ on Graphite, solar cell cover glass, and Kapton. For each of these materials, the model by Kannenberg is used, with a peak yield at 60 degrees, linear energy dependence, zero threshold, and a ratio of peak yield to yield at normal incidence of 2.5. The ratio 2.5 is taken as an average from models and experiments collected by Boyd and Falk.[7] The yields at normal incidence for Kapton and cover glass are taken from measurements performed at NASA: 0.005 and 0.037 units/ion, respectively.[8] The yield at normal incidence for Graphite, .08 units/ion, is taken from Rosenberg and Wehner.[9] Fig. 2 shows the sputter yield versus incidence angle at 300eV. Yield of silvered Teflon (AGT5) and multilayer insulation (MLI) was assumed to be identical to Kapton, since data was not available. Yield

for stainless steel (STAINLESS) and aluminum (AL) was scaled linearly with energy from yields of iron and aluminum, due to Argon at 500eV. The yield of quarts was taken from measurements of solar cell sputtering during an SPT-140 test.[8]

For the two existing plasma simulations, PRESCRIBED_PLUME and RAY, redeposition is calculated by ray tracing. The sputtered flux is distributed as the cosine of the off-normal angle and projected from the sputtering elements to all other viewable surface elements. More detailed models will replace this simple model in the future.

Sputtered material may be deposited on surfaces exposed to the ion beam. There, the deposited material may be re-sputtered onto other surfaces, as shown in Fig. 3. This re-sputtering process may be very important because, for certain geometries, it may influence the type and thickness of re-deposited material on a large percentage of the surface.

For the two existing plasma simulations, PRESCRIBED_PLUME and RAY, an algorithm has been developed to model re-sputtering, and iteratively calculate net sputtering and deposition rates at all surface nodes. Fig. 4 shows a flow description of the algorithm.

The algorithm starts by zeroing the total deposition rate of all materials to all nodes. Then, it calculates the new total deposition rate at each node for each material type. On the

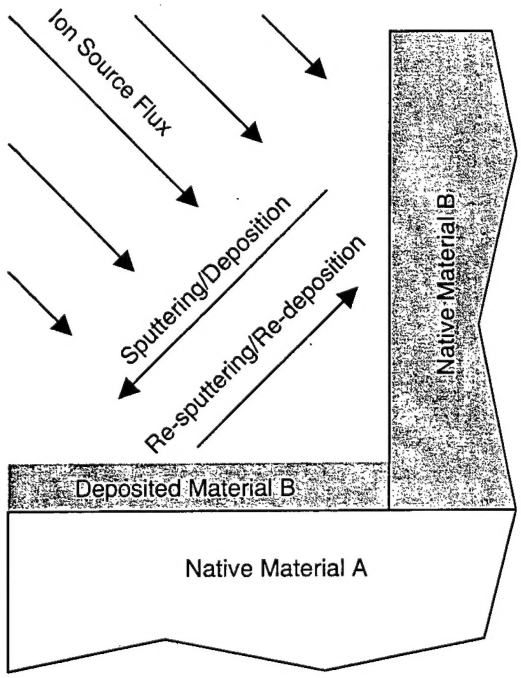

Fig. 3. Illustration of sputtering, deposition, re-sputtering, and re-deposition for a simple geometry with two materials: material A and B, where material B has higher sputter yield than material A.

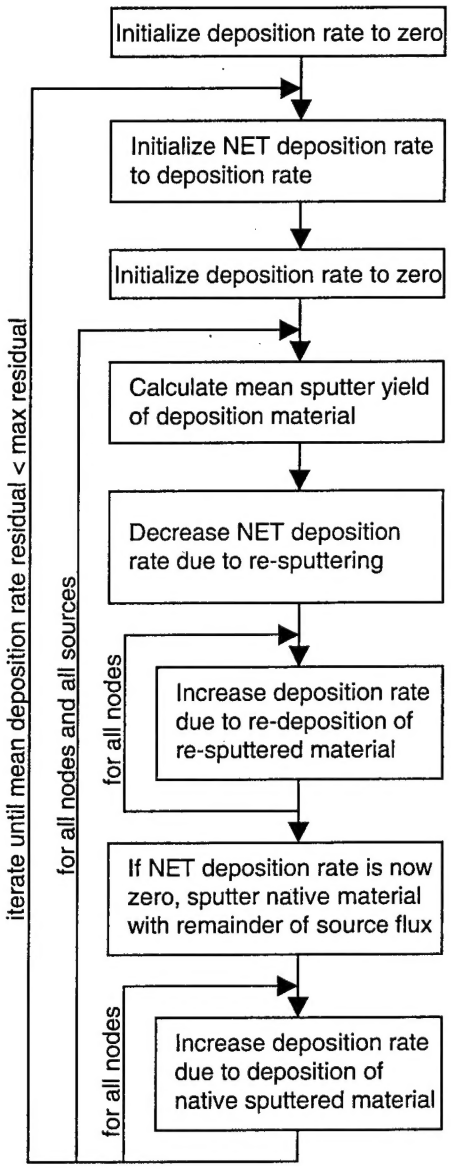

Fig. 4. Flow diagram for the re-sputtering algorithm.

second and subsequent iteration, the algorithm again calculates the new total deposition rate, but takes into account the deposition from the previous iteration. This process is repeated until equilibrium, defined as the mean residual of the net deposition rate reaching some maximum value.

Specifically, deposition from the previous iteration is taken into account by first storing the total deposition rate from the last iteration into a "net" deposition rate variable. As the various sputtering sources (such as ion beams) are considered, this net deposition rate is successively depleted. If and when the net deposition rate becomes zero at a given node, the algorithm begins depleting the native material.

```
# coliseum.in
#
# Load the Chamber 6 geometry,
# superimpose the 200W HET plume
# calculation by SAIC, calculate
# the flux and net sputtering using
# ray tracing, and save the
# results in Tecplot format.
#

material_load material.txt mat_mat.txt

component_load component.txt

surface_load ANSYS Chamber6.ANS

prescribed_plume_load 2DCIRC
 plume_SAIC_200W.dat 0.0 0.0 0.0 0.0 0.0 1.0

ray DEPOSIT 5

surface_save TECPLOT Chamber6.dat
  FLUXNORMAL.XE+ SPUTTERRATE
```

Fig. 5 Sample COLISEUM command file

By "depleting", what is meant is that the surface deposition rate is decreased (or native material sputter rate is increased), and this material is projected to all other nodes as deposition (in the case of native material sputtering) or redeposition (in the case of deposited material). When material is projected to all other nodes, the total deposition rate is increased by the appropriate amount in accordance with the cosine sputtering law mentioned earlier.

One key assumption is that the sputter yield of the "composite" deposition material, which may be made up of many different materials, is the mean of the arriving material sputter yields, weighted by their fluxes:

$$\bar{Y} = \frac{\sum_k Y_k \Gamma_{D,k}}{\sum_k \Gamma_{D,k}} \qquad (1)$$

Above, Y is the sputter yield, and Γ_D is the normal component of the deposition flux, and k is the index of the arriving material. When re-sputtering the deposited material, the above assumption requires that the re-sputtered flux of each material be:

$$\Gamma_{R,k} = \bar{Y}\Gamma_S \frac{\Gamma_{D,k}}{\sum_k \Gamma_{D,k}} \qquad (2)$$

Where Γ_S is the flux of source particles normal to the surface. This ensures material conservation and preserves the ratio of constituents of the composite deposition material.

User Interface

The user enters commands via a COLISEUM input file. The commands are executed sequentially as they appear in the input file. Each command may have some number of parameters separated by spaces or commas. A sample input file is shown in Fig. 5.

Geometry definition typically takes approximately 4 hours for medium-complexity geometries. Typical run times for low-fidelity cases (using PRESCRIBED_PLUME or RAY) take approximately 20 minutes on a 2 GHz Intel Pentium 4 workstation. Once more detailed physics are incorporated, with plasma simulation modules incorporating such algorithms as PIC-DSMC, run times are expected to be between 20 minutes and 20 hours, depending on the level of fidelity and on the initial conditions.

This illustrates a key benefit of using COLISEUM. From scratch, a user can define a complete three-dimensional problem, and generate a first order solution all in less than one workday. Then, for higher fidelity solutions, the problem does not have to be redefined. Then, since the plasma simulation modules are interchangeable, a higher-fidelity algorithm may be immediately started for an overnight run.

Results and Discussion

For the results presented here, COLISEUM, runs were executed for two cases: A) an HET firing inside a laboratory vacuum chamber, and B) a fictitious geosynchronous satellite with an HET firing in the north direction (as if for stationkeeping). Case A is an attempt to validate the sputtering models, and case B is a generalized application to a fictitious spacecraft problem. In both cases, the simple plasma simulation module, PRESCRIBED_PLUME, was used to incorporate a previously calculated plume expansion model onto the surface geometry. The plume expansion model used here was calculated for a Busek 200-Watt HET[10] by SAIC using the GILBERT[3,11] toolbox. Comparisons of this plume model with experiment can be found in a paper by Gardner et al.[12]

Case A

Results from case A are shown in Fig. 6 through Fig. 11. Fig. 8 shows the geometry of a test performed at AFRL. Inside a vacuum chamber, the Busek 200W engine was mounted horizontally on the chamber centerline. A horizontal aluminum table covered with Kapton was mounted 0.188m below the engine. Samples of Kapton and other materials, each approximately 1 cm^2 were placed in rows on the table at varying distances from the thruster exit plane. The chamber walls were stainless steel, but graphite panels were attached to the wall 1.36 meters from the engine face.

Before and after a 100-hour engine firing at 250V and 830mA discharge, the Kapton samples were weighed and their thickness was measured. The differences in sample mass agreed well with the differences in sample thickness (using a Kapton density of 1.42 g/cc).

Fig. 9 shows the orientation of the plume generated by the 200-Watt HET plume. Plasma density is highest near the HET exhaust, and drops off rapidly as the plume expands into the test section.

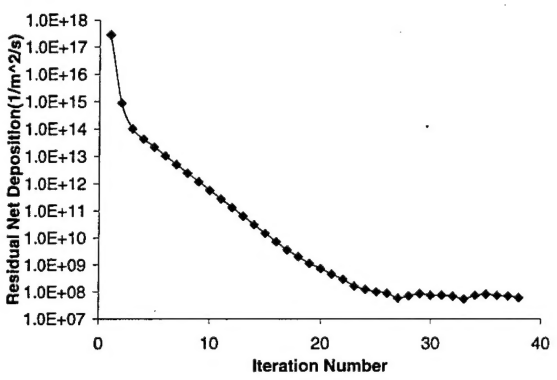

Fig. 6. Convergence of the residual of the mean net deposition rate versus iteration number for the laboratory test case.

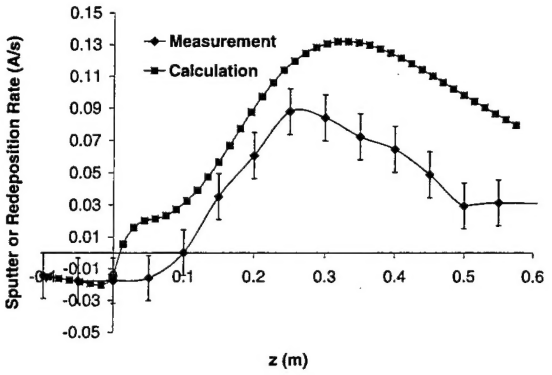

Fig. 7. Comparison between measured and calculated sputtering/deposition rates of Kapton samples. (x=0m, y=-0.188m). Negative values represent net deposition.

Fig. 6 shows, for case A, the convergence properties of the re-sputtering algorithm presented in the previous section. As can be seen from the figure, the mean residual of the net deposition rate decreases exponentially with the number of iterations. For geometries with around 1500 surface elements, like case A, convergence to machine precision typically occurs after approximately 25 iterations.

Fig. 10 and Fig. 11 show the resulting net sputtering and deposition rates, respectively. The net sputtering peaks on the Kapton-covered table where the incidence angle of the ion beam is approximately 60 degrees. This is due to two effects – increased xenon ion flux at that point, and the model for Kapton sputtering yield, which also peaks at approximately 60 degrees. The highest sputtering values are predicted on the aluminum samples, since the sputter yield of aluminum is believed to be much higher than that of Kapton. The net graphite deposition rate peaks on the engine face. On the table, most of the deposited graphite is "cleaned" from the surfaces by the plume. In the area behind the engine exit plane, deposition occurs on the table because ion fluxes are assumed to be zero in this region; thus, "cleaning" does not occur there.

Fig. 7 compares the measured and calculated values of Kapton sputtering/redeposition on the table. Two calculated values are shown – one in which redeposition is not considered, and another with redeposition.

Negative values indicate net deposition of Graphite that was sputtered from the panels. Net deposition can be seen for z<.1m in the measurements, and z<0m in the calculation. This area is underneath the HET, and behind the plume impingement region. Therefore, very little ion flux exists to "clean" away deposited graphite.

Comparing the two calculated results in Fig. 7, one can see the effect of redeposition on the net sputtering rate. For this geometry, redeposition lowers the net sputtering rate by 10% on average. This is due to the competing process of Graphite deposition, and results in a lower net sputtering rate of Kapton. Ion sputtering dominates on the Kapton-covered table. In areas where the ion beam flux is lower, re-sputtering will have a greater influence.

Also in Fig. 7, one can see that the measured and calculated net sputtering rate of Kapton differ by up to a factor of 3. Some possible explanations are: a) our model for Kapton sputtering is high, b) the 200W HET plume model differs from the real case, or c) additional surface effects due to the deposition of graphite effectively harden the surface. This is an area for continued investigation.

Table 1. Additional comparisons of sputter samples exposed during 100-hour chamber test.

z (m)	x (m)	Material	S_{meas} (A/s)	S_{calc} (A/s)
-0.1	0.07	AL	TBD	TBD
0.1	0.07	AL	TBD	TBD
0.3	0.07	AL	TBD	TBD
0.5	0.07	AL	TBD	TBD
-0.1	-0.04	QUARTZ	TBD	TBD
0.1	-0.04	QUARTZ	TBD	TBD
0.3	-0.04	QUARTZ	TBD	TBD
0.5	-0.04	QUARTZ	TBD	TBD
-0.1	-0.08	MLI	TBD	TBD
0.1	-0.08	MLI	TBD	TBD
0.3	-0.08	MLI	TBD	TBD
0.5	-0.08	MLI	TBD	TBD

Sputtering of other samples on the table were also measured and compared with COLISEUM predictions. Some typical values from those comparisons are given in Table 1. The values z and x are the distance from the thruster exit plane and the distance from the table centerline, respectively. The

values S_{meas} and S_{calc} are the measured and calculated sputter rates, respectively.

Case B

Results from case B are shown in Fig. 12 through Fig. 15. Fig. 12 shows the geometry of a generalized geosynchronous satellite. Fig. 13 shows a cross-section of a superimposed HET plume, pointing north. Plasma density is highest near the HET exhaust, and drops off rapidly as the plume expands upward toward the solar arrays.

Sputter rate was calculated using the models presented above, and is shown in Fig. 14. The total rate of redeposition of solar array coverglass is shown in Fig. 15.

Although the net sputtering rate peaks on the radiator wing, most of the total sputtering occurs on the north solar panel and on its concentrators. This illustrates a real problem with electric propulsion on geosynchronous satellites. For north-south stationkeeping, the ideal firing direction (from a thrust efficiency standpoint) is directly north. However, the simulations shows that long-term firing of the HET over the lifetime of a satellite in this configuration may remove a significant amount of material from the spacecraft. In reality, the solar array will be rotating to track the sun, and will not always be positioned directly in the HET plume. Furthermore, the HET would probably be tilted away from due north to reduce plume impingement. Thus, the configuration presented here can be considered a worst case.

Redeposition of sputtered solar array cover glass, shown in Fig. 15, illustrates another potential problem in using EP onboard spacecraft. During HET firing, sputtered material from the solar panels may accumulate on radiator panels, reflectors, or other sensitive surfaces. At the rates predicted here, the emissivity of the material on top (North) of the spacecraft could be changed.

Conclusions

Although still in an early stage of development, COLISEUM now can help predict ion flux and equilibrium net sputtering and deposition rate of surface materials both onboard spacecraft and in laboratory test facilities. COLISEUM's modular architecture is allowing rapid expansion of its capabilities, and giving users flexibility to design their own geometries and choose their preferential plasma simulation method.

The model presented here overpredicts net sputtering rate of Kapton for the geometry tested. Some possible causes are a) our model for Kapton sputter yield is high by a factor of up to 4, b) the 200W HET plume model differs from the real case, or c) additional surface-hardening may be taking place due to the deposition of graphite.

Additional work for the future includes further investigation of the re-sputtering process, further validation against experimental data, and construction of new plasma simulation modules that can self-consistently compute plasma expansion and interaction with surfaces.

References

[1]Kim, V., et al., "Electric Propulsion Activities in Russia," IEPC-01-005, 27th International Electric Propulsion Conference, 2001.

[2]Boyd, I. D., "A Review of Hall Thruster Plume Modeling," AIAA-00-0466, AIAA Aerospace Sciences Conference, 2000.

[3]Gardner et al., "Hall Current Thruster Plume Modeling: A Diagnostic Tool for Spacecraft Subsystem Impact," AIAA-2001-0964.

[4]Mikellides, I.G., et al., "A Hall-Effect Thruster Plume and Spacecraft Interactions Modeling Package," IEPC-01-251, 27th International Electric Propulsion Conference, 2001.

[5]Roussel et al., "Numerical Simulation of Induced Environment, Sputtering and Contamination of Satellite due to Electric Propulsion," Proc. Second European Spacecraft Propulsion Conf. 1997.

[6]K. Kannenberg, V. Khayms, S. H. Hu, B. Emgushov, L. Werthman, and J. Pollard "Validation of a Hall thruster plume sputter model," Paper AIAA-2001-3986, 37th Joint Propulsion Conference, 8-11 July 2001, Salt Lake City, Utah.

[7]Boyd, I. D. and Falk, M. L., "A Review of Spacecraft Material Sputtering by Hall Thruster Plumes," AIAA Paper 2001-3353, 37th Joint Propulsion Conference, Salt Lake City, Utah, 8-11 July 2001.

[8]Fife, J. M. et al., "Spacecraft Interaction Test Results of the High Performance Hall System SPT-140," AIAA-2000-3521, 36th AIAA Joint Propulsion Conference, Huntsville, Alabama, 17-19 July 2000.

[9]Rosenberg, D. amd Wehner, G. K., "Sputtering Yields for Low Energy He+, Kr+, and Xe+ Ion Bombardment," Journal of Applied Physics, Vol. 33, 1962, pp. 1842-1845.

[10]V. Hruby, J. Monheiser, B. Pote, C. Freeman, and W. Connolly, "Low Power, Hall Thruster Propulsion System," IEPC-99-092, 26th International Electric Propulsion Conference, 17-21 October, 1999, Kitakyushu, Japan

[11]Katz et al, "A Hall Effect Thruster Plume Model Including Large-Angle Elastic Scattering," AIAA-2001-3355, 37th Joint Propulsion Conference, Salt Lake City, Utah, 8-11 July 2001.

[12]Gardner et al., "Assessment of Spacecraft Systems Integration Using the Electric Propulsion Interactions Code," AIAA-2002-3667, 38th AIAA/ASME/SAE/ASEE Joint Propulsion Conference, Indianapolis, Indiana, 2002.

CASE A – Laboratory Experiment with 200W HET

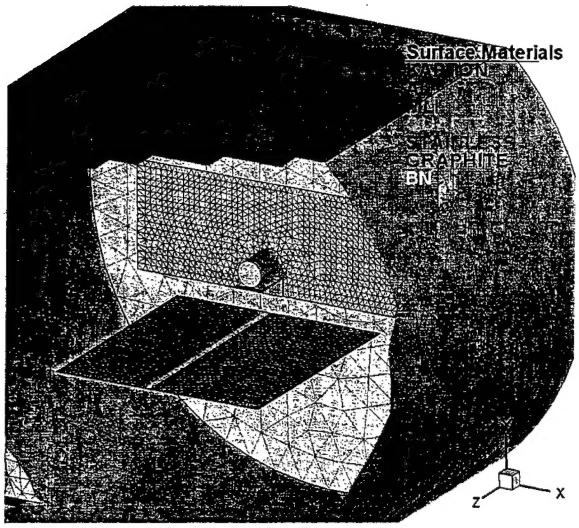

Fig. 8. Cutaway of an HET test setup showing the HET, a horizontal Kapton-covered table, and graphite panels placed on the vacuum chamber walls.

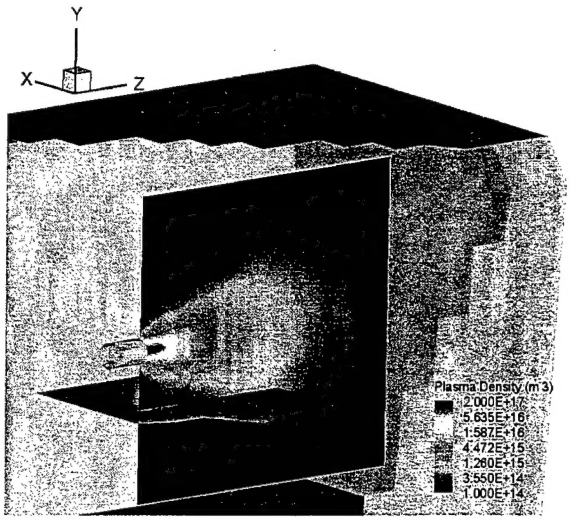

Fig. 9. Slice showing the orientation of the thruster plume and approximate plasma density values.

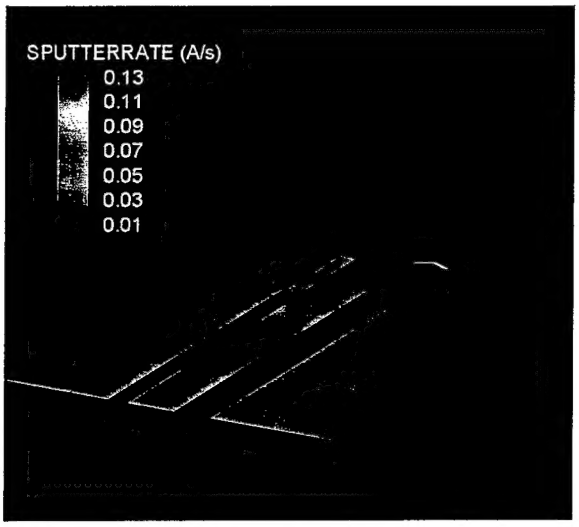

Fig. 10. Net surface sputtering rate. Negative values indicate net deposition.

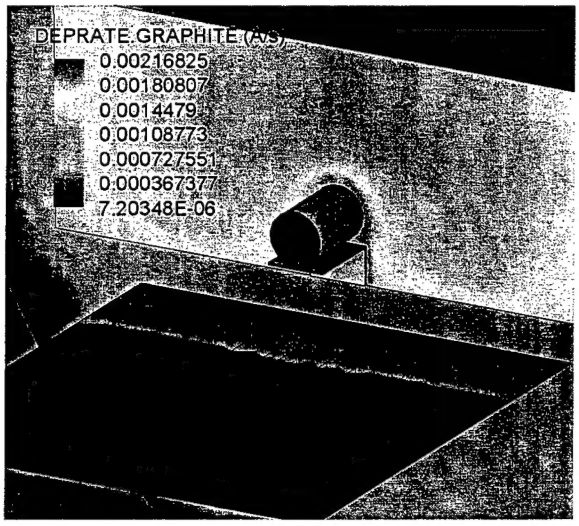

Fig. 11. Net deposition rate of graphite.

CASE B – Geosynchronous Satellite with HET for North-South Stationkeeping

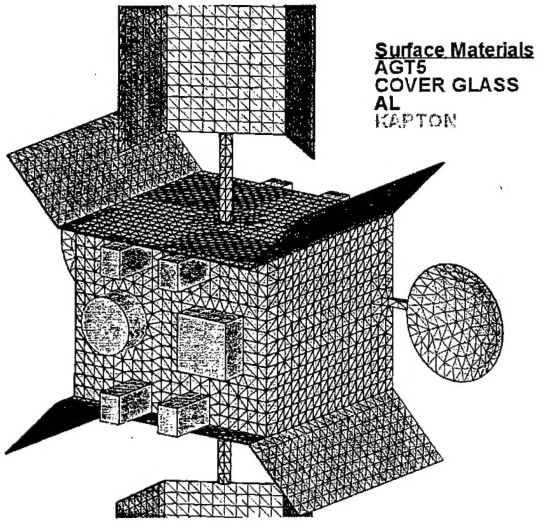

Fig. 12. Surface mesh of a geosynchronous satellite geometry with eight HETs positioned for north-south stationkeeping.

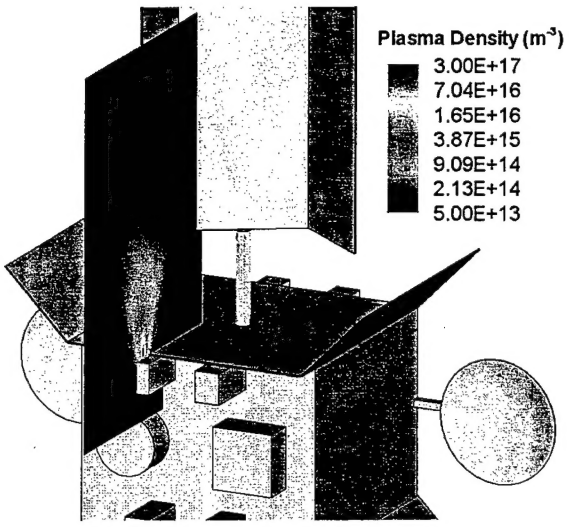

Fig. 13. Slice showing plasma density from a 200-Watt HET firing onboard a geosynchronous satellite.

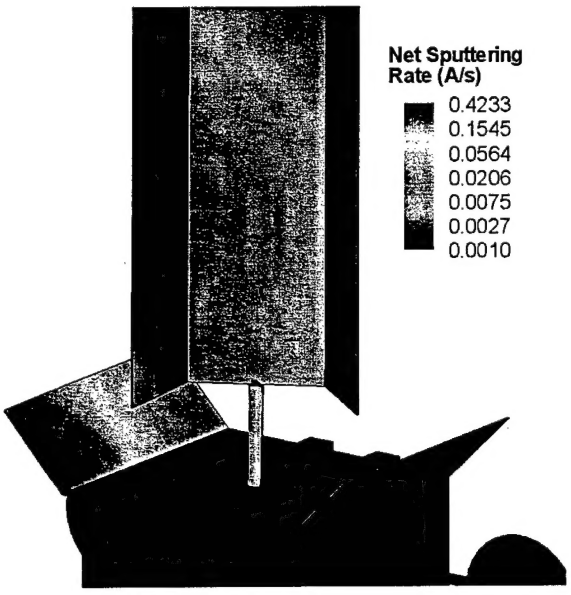

Fig. 14. Net surface sputtering rate.

Fig. 15. Total redeposition rate of ITO from the solar array cover glass to other spacecraft surfaces due to sputtering.